

Synthesis, Biological Evaluation, and Structure–Activity Relationships of a Novel Class of Apurinic/Apyrimidinic Endonuclease 1 Inhibitors

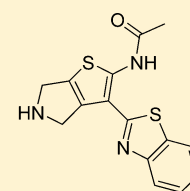
Ganesha Rai,^{†,§} Vaddadi N. Vyjayanti,^{‡,§} Dorjbal Dorjsuren,[†] Anton Simeonov,[†] Ajit Jadhav,[†] David M. Wilson, III,^{*,‡} and David J. Maloney^{*,†}

[†]NIH Chemical Genomics Center, National Center for Advancing Translational Sciences, National Institutes of Health, Bethesda, Maryland 20892-3370, United States

[‡]Laboratory of Molecular Gerontology, National Institute on Aging, National Institutes of Health, Baltimore, Maryland 21224, United States

Supporting Information

ABSTRACT: APE1 is an essential protein that operates in the base excision repair (BER) pathway and is responsible for $\geq 95\%$ of the total apurinic/apyrimidinic (AP) endonuclease activity in human cells. BER is a major pathway that copes with DNA damage induced by several anticancer agents, including ionizing radiation and temozolomide. Overexpression of APE1 and enhanced AP endonuclease activity have been linked to increased resistance of tumor cells to treatment with monofunctional alkylators, implicating inhibition of APE1 as a valid strategy for cancer therapy. We report herein the results of a focused medicinal chemistry effort around a novel APE1 inhibitor, *N*-(3-(benzo[*d*]thiazol-2-yl)-6-isopropyl-4,5,6,7-tetrahydrothieno[2,3-*c*]pyridin-2-yl)acetamide (3). Compound 3 and related analogues exhibit single-digit micromolar activity against the purified APE1 enzyme and comparable activity in HeLa whole cell extract assays and potentiate the cytotoxicity of the alkylating agents methylmethane sulfonate and temozolomide. Moreover, this class of compounds possesses a generally favorable *in vitro* ADME profile, along with good exposure levels in plasma and brain following intraperitoneal dosing (30 mg/kg body weight) in mice.



compound 52

INTRODUCTION

Apurinic/apyrimidinic (AP) endonuclease 1 (APE1) is the primary mammalian enzyme responsible for the removal of abasic (or AP) sites in DNA.^{1,2} Such lesions can arise as products of the repair activity of DNA glycosylases, which carry out the first step of base excision repair (BER), or as products of spontaneous or damage-induced hydrolysis of the *N*-glycosidic bond that links the base to the sugar moiety of the phosphodiester DNA backbone. APE1 initiates AP site repair by catalyzing a Mg²⁺-facilitated strand incision event immediately 5' to the lesion, leaving behind a single-strand break with a normal 3'-hydroxyl residue and a 5'-abasic fragment. Other proteins of BER, such as DNA polymerase β and DNA ligase 3, complete the repair response by removing the remaining abasic residue, replacing the missing nucleotide, and sealing the nick.³ Besides being the predominant repair enzyme for AP sites in DNA, APE1 also possesses repair nuclease activities against various nonconventional 3'-blocking terminal groups, such as phosphoglycolates, phosphates, and chain-terminating nucleoside analogues.⁴ In addition, APE1 has roles in regulating gene expression, most notably through its capacity to modulate the DNA binding activity of several transcription factors, e.g., AP-1, p53, and NF- κ B, via a less well understood redox mechanism.^{5–7}

APE1 protein levels and intracellular distribution have been correlated with cancer type and stage, as well as responsiveness to clinical DNA-damaging agents, such as the alkylator

temozolomide (TMZ).^{8,9} TMZ is a promising drug recently added to the arsenal of alkylating agents for the adjuvant chemotherapy of brain cancers because of its ability to readily cross the blood–brain barrier.¹⁰ It has therefore been postulated that APE1 would be an attractive target in anticancer treatment paradigms involving coadministration with certain DNA-interactive drugs, where strategic regulation of its repair activity would improve the therapeutic efficacy and clinical outcome.

Targeting DNA repair enzymes as single-agent cancer therapy has been validated as a viable strategy by the discovery and clinical evaluation of poly ADP-ribose polymerase (PARP) inhibitors.¹¹ PARP1 is an enzyme that facilitates efficient repair of single-strand breaks in DNA. Thus, inhibition of PARP1 leads to the accumulation of one-ended double-strand DNA breaks upon replication fork collapse that are ultimately repaired via homologous recombination (HR).¹² BRCA1/2 are proteins involved in the HR pathway, and consequently, treatment of BRCA-deficient cancer cells (e.g., ~ 10 –20% of triple negative breast cancers) with PARP1 inhibitors leads to irreparable DNA damage and ultimately cell death.¹³ This synthetic lethal relationship offers the prospect of selective targeting of cancer cells, since normal cells would maintain the ability to repair DNA double-strand breaks. However, despite

Received: November 14, 2011

Published: March 28, 2012

continued efforts and promising results in this area of research, the use of PARP1 inhibitors has not been without its recent setbacks in the clinic.¹⁴ While synthetically lethal combinations involving APE1 inhibitors have not yet been established, it is not unreasonable to postulate the use of APE1 inhibitors as single agent therapy by such a mechanism.

As a result of the promising therapeutic potential of this target, several reports have described the identification and characterization of small molecules that inhibit APE1 repair endonuclease activity.¹⁵ Kelley and co-workers described the identification of 2,4,9-trimethylbenzo[*b*][1,8]naphthyridin-5-amine, **1** (AR03) through a fluorescence-based high-throughput screen (HTS) of 60 000 compounds (Figure 1).¹⁶ **1** was found

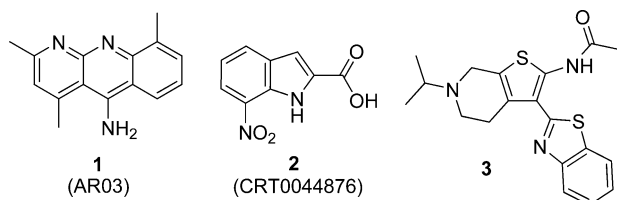


Figure 1. Previously reported APE1 endonuclease inhibitors (**1** and **2**) and the lead chemotype (**3**).

to have low micromolar in vitro potency against purified human APE1 and inhibited AP site incision activity of whole cell extracts and the repair of AP sites in SF767 glioblastoma cells. Moreover, **1** potentiated the cytotoxicity of methyl methanesulfonate (MMS) and TMZ in SF767 cells. 7-Nitro-1*H*-indole-2-carboxylic acid, **2** (CRT0044876) (Figure 1), was identified by Madhusudan et al. in 2005, and they described specific inhibition of the exonuclease III family of AP endonucleases and the induction of AP sites in HT1080 fibrosarcoma cells.¹⁷ While a synergistic cell killing effect was seen with the inhibitor when combined with MMS or TMZ, other subsequent studies have been unable to reproduce the potentiating effect of **2**.¹⁸ More recently, Madhusudan and colleagues described the results of a virtual screen of 2.6 million compounds from which several low micromolar APE1 inhibitors were found.¹⁹ Other reported APE1 inhibitors include the bis-carboxylic acid containing small molecules described by Zawahir et al.,²⁰

lucanthone (also a topoisomerase inhibitor),²¹ methoxyamine,²² and various arylstibonic acids.²³

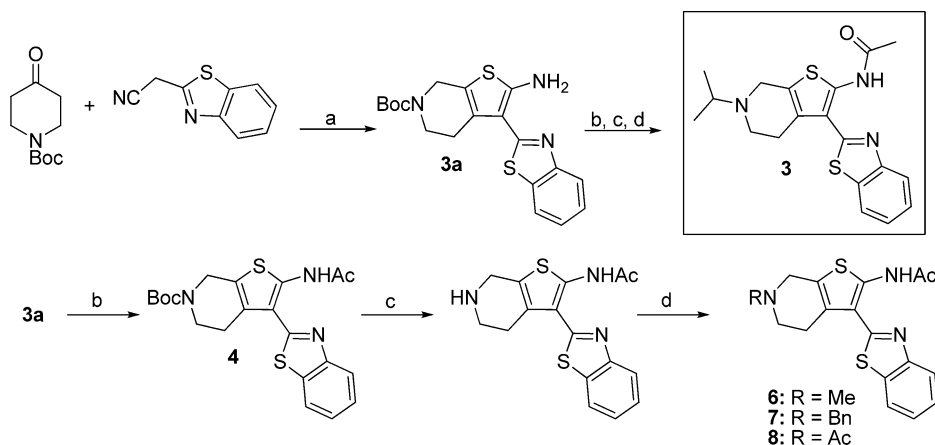
We recently reported on the development of a 1536-well fluorescence-based, quantitative HTS (qHTS) assay, which was used to screen the Library of Pharmacologically Active Compounds (LOPAC¹²⁸⁰) for novel APE1 endonuclease inhibitors.²⁴ This library is a collection of well characterized bioactive molecules that is often used to help validate an assay platform before screening of an entire small molecule collection. Our initial efforts identified several compounds, including 6-hydroxy-DL-DOPA, reactive blue, and myricetin, which inhibit AP site cleavage activity of purified APE1, as well as HEK293T and HeLa whole cell extracts, and exhibit potentiating effects of MMS toxicity. These prior studies established general methods for identification and validation of APE1 inhibitors. While encouraged by these results, we were eager to identify novel small molecule inhibitors that would represent an improved starting point for medicinal chemistry optimization, as the three LOPAC¹²⁸⁰ compounds mentioned above appear to be generally promiscuous given the broad publications on their various modes of action.

As such, we conducted a large-scale qHTS in a 1536-well concentration response format on our complete in-house collection, which at the time contained 352 498 small molecules²⁵ as part of the NIH Molecular Libraries Small Molecule Repository (MLSMR). This effort represents the largest reported screening campaign against APE1 thus far and led to the identification of several novel chemotypes displaying potent inhibition of APE1 activity. In this report, we discuss the synthesis, biological characterization, and structure–activity relationship (SAR) of one of the molecules, *N*-(3-(benzo[*d*]thiazol-2-yl)-6-isopropyl-4,5,6,7-tetrahydrothieno[2,3-*c*]pyridin-2-yl)acetamide (**3**) (Figure 1). This compound, along with related analogues, displayed low micromolar APE1 inhibition and activity in HeLa whole cell extract assays, potentiated the cytotoxicity of MMS and TMZ, and led to a hyperaccumulation of AP sites in HeLa cells treated with MMS.

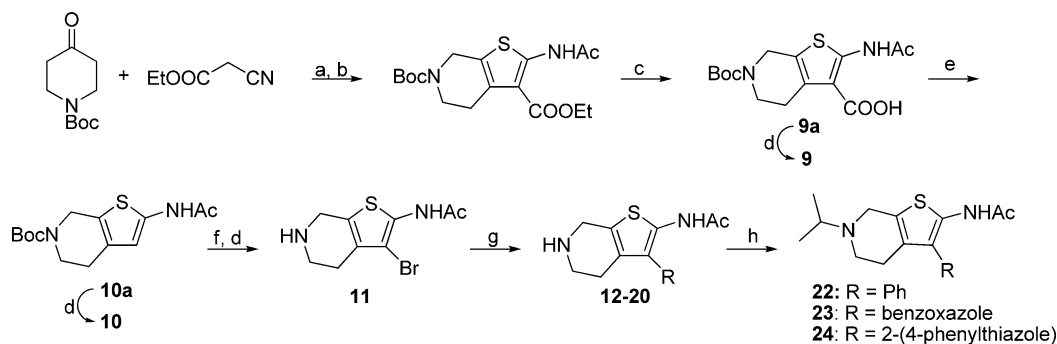
CHEMISTRY

The synthesis of the lead chemotype **3** from the qHTS campaign commenced with treatment of commercially available

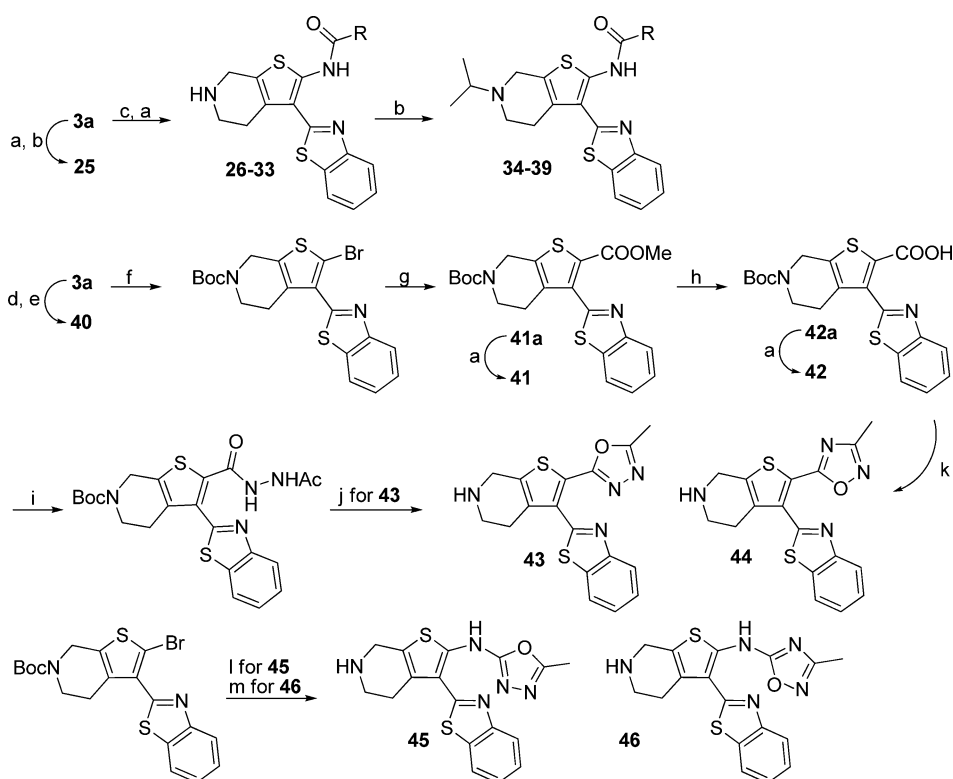
Scheme 1. Synthesis of qHTS “Hit” **3** and Related Analogues **4**–**8**^a



^aReagents and conditions: (a) S, morpholine, EtOH, reflux, 2 h (87%); (b) AcCl, Hunig's base, CH₂Cl₂, rt, 1 h (91%); (c) TFA, CH₂Cl₂, rt, 1 h (99%). (d) **3**: acetone, NaCNBH₃, MeOH/THF, rt, 6 h (75%). **6**: paraformaldehyde (aq), NaCNBH₃, MeOH/THF, rt, 6 h. **7**: PhCHO, NaCNBH₃, MeOH/THF, 6 h. **8**: AcCl, Hunig's base, CH₂Cl₂, rt.

Scheme 2. Synthesis of Analogues 9–24^a

^aReagents and conditions: (a) S, morpholine, EtOH, reflux, 2 h (84%); (b) AcCl, Hunig's base, CH₂Cl₂, rt, 1 h (91%); (c) LiOH, THF/H₂O, reflux, 24 h (65%); (d) TFA, CH₂Cl₂, rt, 0.5 h; (e) dimethylacetamide, 170 °C, microwave, 2 h (77%); (f) Br₂, CHCl₃, -10 °C, 1 h (70%); (g) R-B(OH)₂, Pd(PPh₃)₄, Na₂CO₃, DME, 150 °C, microwave, 0.5–1.5 h; (h) acetone, NaCNBH₃, MeOH/THF, rt, 6–10 h.

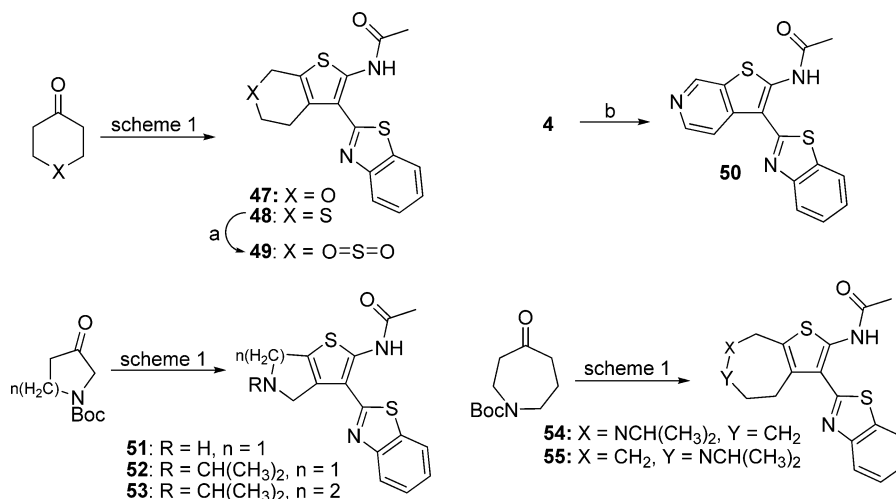
Scheme 3. Synthesis of Analogues 25–46^a

^aReagents and conditions: (a) TFA, CH₂Cl₂, rt, 0.5 h; (b) acetone, NaCNBH₃, MeOH, rt, 6 h; (c) RC(O)Cl, (*i*-Pr)₂NEt, CH₂Cl₂, rt, **31**, **33**, **36**: RC(O)OH, EDC, DMAP, DMF, rt, 1 h, (85–90%). (d) NaNO₂, HCl–H₂SO₄, 0 °C, 2 h; (e) H₃PO₂, rt, 1 h; (f) *t*-BuNO₂, CuBr₂, MeCN, 0 °C → rt, 4 h; (g) Pd(OAc)₂, dppp, CO_(g) (1 atm), NEt₃, DMSO–MeOH (1:1), 60 °C, 24 h, (69%); (h) LiOH, THF/MeOH/H₂O (6:2:1), rt, 3 h (91%); (i) acetohydrazide, EDC, DMF, rt, 2 h (97%); (j) Burgess reagent, THF, 100 °C, microwave, 0.5 h (73%), then TFA, CH₂Cl₂, rt, 0.5 h; (k) *N*'-hydroxyacetimidamide, HATU, (*i*-Pr)₂NEt, 50 °C for 15 min, then 150 °C for 15 min, microwave, 1 h, then TFA, CH₂Cl₂, rt, 0.5 h; (l) 5-methyl-1,3,4-oxadiazol-2-amine, Pd₂(dba)₃, xantphos, Cs₂CO₃, dioxane, 125 °C, microwave, 2 h, then TFA, CH₂Cl₂, rt, 0.5 h; (m) 3-methyl-1,2,4-oxadiazol-5-amine, Pd₂(dba)₃, xantphos, Cs₂CO₃, dioxane, 125 °C, microwave, 2 h, then TFA, CH₂Cl₂, rt, 0.5 h.

N-(Boc)-4-piperidone with 2-benzothiazoleacetonitrile in the presence of elemental sulfur and morpholine to afford the key intermediate **3a** as shown in Scheme 1.²⁶ Acetylation of the 2-amino group, followed by Boc deprotection with trifluoroacetic acid (TFA) and reductive amination with acetone and NaCNBH₃, gave the desired compound **3** in good yield. Starting with intermediate **3a**, several different *N*-substituted analogues were synthesized, including R = Me (**6**, via reductive amination with paraformaldehyde), R = Bn (**7**) (via reductive

amination with benzaldehyde), and R = Ac (**8**, via acylation with AcCl).

The synthesis of analogues **9–24**, which involved modification to the C-3 benzothiazole ring, required the development of a more convergent route. While the original synthesis of lead compound **3** only involved four steps, diversity of the benzothiazole ring occurs in the first step and thus requires the availability of the necessary acetonitrile derivative. Moreover, each modified benzothiazole analogue would involve a

Scheme 4. Synthesis of Analogues 47–55^a

^aReagents and conditions: (a) *m*-CPBA, CH₂Cl₂, 0 °C, 1 h, (87%); (b) MnO₂, toluene, 120 °C, microwave, 10 min (49%).

minimum of four steps, making library synthesis quite laborious. As such, we envisaged a late-stage Suzuki coupling of commercially available boronic acids to the 3-bromothiophene intermediate (**11**) allowing for rapid access to a variety of analogues at the 3-position as shown in Scheme 2. Reaction of *N*-(Boc)-4-piperidone with ethyl 2-cyanoacetate using the conditions described above (*S*, morpholine), followed by acetylation and subsequent saponification of the formed ethyl ester, gave the desired 3-COOH intermediate **9a**. Decarboxylation using dimethylacetamide at 170 °C for 2 h in a microwave gave the des-carboxy product **10a** after optimization of the reaction conditions. Typically, this transformation is carried out with copper using quinoline as the solvent or oxalic acid in isopropanol, both at elevated temperatures. Our conditions are quite mild (albeit at elevated temperatures), and a wide range of functional groups should be tolerated. Subsequent bromination of **10a** using Br₂ in chloroform at –10 °C followed by Boc deprotection gave **11** in good yield. Importantly, we found that the late-stage Suzuki coupling could be accomplished using the unprotected piperidine moiety via treatment of **11** with various commercially available boronic acids to provide **12–20** in good yields. Reductive amination with acetone, NaCNBH₃, and MeOH/THF as the solvent gave the *N*-isopropyl analogues **22–24**.

Analogues **25–46** were synthesized in an effort to further understand the SAR of the amide moiety as shown in Scheme 3. Analogue **25**, in which the 2-amino group was left unacetylated, was prepared in two steps from the common intermediate **3a** via Boc deprotection and regioselective reductive amination of the piperidine moiety with acetone and NaCNBH₃. Analogues **26–33**, involving either reaction with the requisite acid chloride or EDC-mediated peptide coupling conditions (for **31**, **33**, and **36**), were utilized to afford the desired products in good yields. In addition to the various amide analogues, we wanted to investigate amide bioisosteres such as oxadiazoles **43–46**. The synthesis of oxadiazole analogues **43** and **44** commenced with conversion of the 2-amino group to the corresponding bromide using *tert*-butyl nitrite and copper bromide in acetonitrile. Palladium-catalyzed carboxylation was achieved using catalyst Pd(OAc)₂, catalyst dppp, in DMSO–MeOH under an atmosphere of CO_(g) to afford the desired methyl ester derivative **41a** in 69% yield.

Saponification of **41a** with lithium hydroxide in a THF/MeOH/H₂O mixture gave carboxylic acid **42a** in high yield. Formation of the acylhydrazide was accomplished using acetoacetylhydrazide and EDC in DMF. Dehydrative cyclization was achieved using methyl *N*-(triethylammoniumsulfonyl)-carbamate (Burgess reagent) in THF at 100 °C in the microwave to give, after Boc deprotection (TFA, CH₂Cl₂), the 1,3,4-substituted oxadiazole **43** in good yield. 1,2,4-Oxadiazole derivative **44** was prepared in three steps from intermediate **42a** via treatment with *N*'-hydroxyacetimidamide, HATU, Hunig's base at (50 °C → 150 °C) to afford the cyclized product, which after Boc deprotection gave the desired product **44**. Access to 2-aminooxadiazole analogues **45** and **46** was achieved via Buchwald–Hartwig-type cross-couplings of the requisite commercially available amino oxadiazole (5-methyl-1,3,4-oxadiazol-2-amine (**45**) and 3-methyl-1,2,4-oxadiazol-5-amine (**46**)) using Pd₂(dba)₃, xantphos, and cesium carbonate in the microwave for 2 h followed by Boc deprotection.

As shown in Scheme 4, we were eager to investigate various heteroatoms in place of the piperidine nitrogen of lead compound **3** (e.g., O, **47**; S, **48**; SO₂, **49**). Accordingly, the syntheses of **47** and **48** were carried out in a manner similar to that shown in Scheme 1, except tetrahydropyran-4-one and tetrahydrothiopyran-4-one were used for the preparation of **47** and **48**, respectively. Synthesis of sulfone derivative **49** was accomplished via treatment of **48** with *m*-CPBA in methylene chloride at 0 °C, and pyridine analogue **50** was obtained via MnO₂ oxidation of intermediate **4**. Five-membered ring analogues **51** and **52** were prepared using the route described in Scheme 1 except *N*-Boc-3-pyrrolidinone was used as the starting material, whereas for **53**, *N*-(Boc)-3-piperidone was utilized. Analogues **54** and **55** were synthesized from 1-Boc-4-azepanone, which upon cyclization (*S*, morpholine) gave two separable regioisomers that were easily distinguishable by ¹H NMR; both reactions were carried through using the described sequence to provide the desired products.

RESULTS AND DISCUSSION

SAR Analysis of Compound 3 Using the Fluorescence-Based HTS Assay. As a benchmark, we included some of the previously reported APE1 inhibitors. Specifically, **1** was already part of the MLSMR collection and **2** was purchased from Sigma

Chemical Company. As shown in Table 1, compound 2 showed only modest inhibition (40%) at concentrations up to 57 μM ,

Table 1. Activity of Previously Reported APE1 Inhibitors (1 and 2) and SAR of Analogues 3–8

Compound	R	IC ₅₀ ^a (μM) [\pm SD (μM)]	Inh. @ 57 μM ^b
1	NA	32 ^c	—
2	NA	—	40%
3	CH(CH ₃) ₂	2.0 [0.1]	—
4	H	2.9 [0.1]	—
5	Boc	>57	—
6	Me	3.8 [0.3]	—
7	Bn	—	41%
8	Ac	—	59%

^aIC₅₀ values were determined using the qHTS protocol and represent the average of three separate experiments. ^bFor compounds that did not achieve full inhibition (>85%), the % inhibition at the highest tested concentration (57 μM) is noted. Compounds noted as >57 μM are considered inactive. ^cIC₅₀ of this compound reflects data from primary screen; follow-up studies with a powder sample were not further pursued.

in agreement with previous reports that showed an inability to reproduce the activity of this small molecule.¹⁸ 1 did show APE1 inhibition, albeit lower than the reported IC₅₀ value (1.5 μM reported¹⁶ vs 32 μM observed). Since assay variability is to be expected, this observation emphasizes the need to include prior art as internal comparative controls. This result is from the primary screen and not from a synthesized or purified commercial powder source, so the source and effective concentration of the sample could also contribute to the discrepancy. Our lead compound 3 exhibited an IC₅₀ of 2 μM in the qHTS assay (Table 1) and an IC₅₀ of 12 μM in a radiotracer incision assay (RIA). The confirmed activity, chemical tractability, and preliminary cell-based data, which showed that compound 3 potentiated the cytotoxicity of MMS in HeLa cells (vide infra), led us to proceed with optimization and SAR exploration of this chemotype.

Our first SAR investigations involved modification of the piperidine nitrogen moiety, which revealed that acylation was not well tolerated, as introduction of both a Boc group (5) and an acetyl group (8) led to a significant loss of activity. Moreover, the benzyl substituted analogue (7) showed greatly reduced activity with only 41% inhibition at the highest concentration tested (57 μM). In contrast, removal of the isopropyl group (4) and introduction of the smaller alkyl group (R = Me, 6) had little effect on potency with IC₅₀ values of 2.9 and 3.8 μM , respectively. These data suggest that potency is greatly affected by the absence of a basic nitrogen (analogues 5 and 8). However, there is also not much tolerance for larger hydrophobic groups given that the benzyl substituted analogue, which maintains the basic character of the nitrogen, is weakly active.

The next area of SAR exploration involved modification of the benzothiazole moiety at the 3-position of the thiophene. Given the results obtained from our initial round of SAR (Table 1), where we found analogue 4 (lacking isopropyl group) to have potency comparable to that of derivative 3, most analogues were submitted for testing as the free amine to eliminate one step in the analogue synthesis. As shown in Table 2, many of the changes were not productive, with many compounds being inactive or only having modest activity at the highest concentration. Replacing the benzotriazole motif with other heterocycles, including furan (13), thiophene (14),

Table 2. SAR of Analogues 9–24

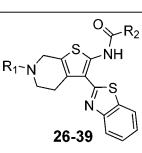
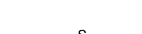
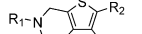
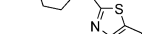
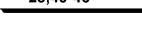
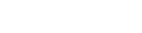
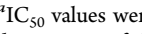
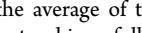
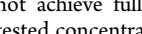
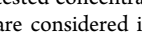
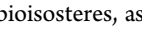
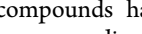
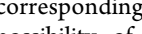
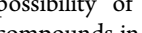
Compound	R ₁	R ₂	IC ₅₀ ^a (μM) [\pm SD (μM)]	Inh. @ 57 μM ^b
9	H	COOH	—	29%
10	H	H	—	47%
11	H	Br	—	30%
12	H	1-naphthalene	>57	—
13	H	2-furan	—	41%
14	H	2-thiophene	—	34%
15	H	2-benzothiophene	—	23%
16	H	3-benzothiophene	>57	—
17	H	2-benzofuran	—	66%
18	H	2-indole	>57	—
19	H	2-oxazole	—	45%
20	H	2-thiazole	—	55%
21	CH(CH ₃) ₂	CN	—	31%
22	H	Ph	—	42%
23	CH(CH ₃) ₂	benzoxazole	20.4 [0.1]	—
24	CH(CH ₃) ₂	NA	2.9 [0.1]	—

^aIC₅₀ values were determined using the qHTS protocol and represent the average of three separate experiments. ^bFor compounds that did not achieve full inhibition (>85%), the % inhibition at the highest tested concentration (57 μM) is noted. Compounds noted as >57 μM are considered inactive.

benzothiophene (15), benzofuran (17), oxazole (19), and thiazole (20), resulted in greatly diminished activity. Similar results were obtained when that position was modified with a simple phenyl group (22) or numerous other substituted phenyl derivatives (data not shown). Interestingly, even the structurally similar benzoxazole analogue (23) had a 10-fold loss in activity; however, the 2-(4-phenylthiazole) analogue (24) displayed potent inhibition with activity comparable to that of the lead compound. The combination of the reduced activity for the benzoxazole derivative (23) and the maintenance of activity for compound 24 suggests that the thiazole motif is involved in an essential interaction with APE1 and should be maintained in some capacity in future analogues. However, additional substitution is required, since the thiazole alone (compound 20) displayed minimal activity. As such, additional modifications of the pendent aryl ring in analogue 24 may prove fruitful.

The goal of analogues 25–46 (Table 3) was to gain a better understanding of the SAR associated with the *N*-acetyl moiety of the lead compound 3. Thus, a variety of different compounds were prepared, including a des-acetyl, numerous amides, carbamates, carboxylic acids, esters, and amide bioisosteres (1,2,4-oxadiazoles and 1,3,4-oxadiazoles). Our first interest was to look at the des-acetyl analogue 25; this modification was clearly unfavorable with only 40% inhibition at 57 μM being observed. Interestingly, compound 25 was less potent than analogue 40, which has the amino group removed altogether. Many of the amide analogues resulted in a decrease in potency [e.g., *tert*-butyl (26), inactive; cyclopentane (28), 55% at 57 μM ; Bn (29), 53% at 57 μM ; (CH₂)₂Ph (30), inactive]. However, other amide analogues exhibited a less pronounced drop in activity [e.g., cyclopropane (27), 6 μM ; cyclohexane (37), 8.3 μM ; CHF₂ (33 and 36), 3.8 and 5.3 μM , respectively]. Replacing the amide with other functional groups, such as carboxylic acid (42) or ester (41), resulted in complete loss of activity; however, methyl carbamate (32) was marginally active with an IC₅₀ of 11 μM . Given the possibility of hydrolysis of the amide by intracellular amidases, we were eager to explore the tolerance of amide bioisosteres such as 1,2,4-oxadiazoles and 1,3,4-oxadiazoles. To this end, both analogues that lack the 2-amino group (43 and 44) and those that maintained this moiety (45 and 46) were investigated. The studies revealed the necessity of the 2-amino group for maintaining activity for these

Table 3. SAR of Analogues 25–46

Compound	R ₁	R ₂	IC ₅₀ ^a (μM) [± SD (μM)]	Inh. @ 57 μM ^b
	CH(CH ₃) ₂	NH ₂	—	40%
	H	C(CH ₃) ₃	>57	
	H	cyclopropane	6.0 [0.4]	
	H	cyclopentane	—	55%
	CH(CH ₃) ₂	Bn	—	53%
	H	(CH ₂) ₂ -Ph	>57	
	H	CF ₃	17.6 [2.4]	
	H	OMe	11.1 [0.7]	
	H	CHF ₂	3.8 [0.3]	
	H	(CH ₂) ₂ -C≡CH	12.0 [0.8]	
	CH(CH ₃) ₂	(CH ₂) ₂ -C≡CH	—	57%
	CH(CH ₃) ₂	CHF ₂	5.3 [0.4]	
	CH(CH ₃) ₂	cyclohexane	8.3 [0.1]	
	CH(CH ₃) ₂	(CH ₂) ₃ -CH ₃	9.1 [0.1]	
	CH(CH ₃) ₂	Ph	—	57%
	H	H	25.2 [1.9]	
	H	C(O)OMe	>57	
	H	COOH	>57	
	H		>57	
	H		>57	
	H		19.0 [1.3]	
	H		18.2 [0.1]	

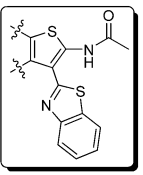
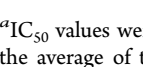
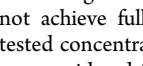
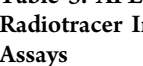
^aIC₅₀ values were determined using the qHTS protocol and represent the average of three separate experiments. ^bFor compounds that did not achieve full inhibition (>85%), the % inhibition at the highest tested concentration (57 μM) is noted. Compounds noted as >57 μM are considered inactive.

bioisosteres, as compounds **43** and **44** were completely inactive while **45** and **46** had modest activity. While these last two compounds have approximately 8-fold less activity than the corresponding amide analogue (**4**), it does suggest the possibility of utilizing such modifications on this class of compounds in later rounds of optimization if deemed necessary by pharmacokinetic (PK) studies.

Our last foray into the SAR characterization described herein involved modification of the piperidine ring, where we replaced the nitrogen with other heteroatoms. In the absence of structural information to guide our medicinal chemistry efforts, we aimed to explore the effect (i.e., altering key hydrogen bond contacts) of moving the nitrogen to different positions on the ring and varying the ring size (e.g., *n* = 5, 6, and 7). As shown in Table 4, most of these changes were met with limited success; however, a few interesting lessons were learned. Replacing the nitrogen with oxygen (analogue **47**) or sulfur (analogue **48**) led to compounds that were still active against APE1, albeit only at the highest concentration. Sulfone derivative **49** had very minimal efficacy (29%), and pyridine analogue **50** was completely inactive. Varying the ring size with pyrrolidine analogues **51** and **52** had a limited effect on activity, with IC₅₀ values of 3 and 3.1 μM, respectively. Differentially substituted piperidine analogue **53** had only modest efficacy at 57 μM, while the seven-membered ring derivatives **54** and **55** displayed activities of 12.9 and 17.6 μM, respectively.

APE1 Inhibition in Radiotracer Incision and HeLa Whole Cell Extract Assays. Having tested all of the synthesized analogues using the fluorescence-based HTS assay to establish a rank order of potency, we next aimed to validate their activity by testing in the RIA. This assay is considered the “golden standard”, but because of its low throughput nature, only our top analogues were analyzed via this method (Table 5). Most analogues had comparable activity across both experimental platforms, with **52** emerging as the most potent compound in the RIA.

Table 4. SAR of Analogues 47–55

Compounds	R	Heterocycle	IC ₅₀ ^a (μM) [± SD (μM)]	Inh. @ 57 μM ^b
	NA		—	41%
	NA		—	56%
	NA		—	29%
	NA		>57	
	CH(CH ₃) ₂		3.1 [0.2]	
	H		3.3 [0.2]	
	H		—	31%
	CH(CH ₃) ₂		12.9 [0.1]	
	CH(CH ₃) ₂		17.6 [1.1]	

^aIC₅₀ values were determined using the qHTS protocol and represent the average of three separate experiments. ^bFor compounds that did not achieve full inhibition (>85%), the % inhibition at the highest tested concentration (57 μM) is noted. Compounds noted as >57 μM are considered inactive.

Table 5. APE1 Inhibition of Select Compounds in Radiotracer Incision, HTS, and HeLa Whole Cell Extracts Assays

compd	RIA IC ₅₀ ^a (μM)	HTS IC ₅₀ (μM)	HeLa cell extract, % incision activity ^b
3	12	2.0	0.6 ± 0.11
4	5	2.9	1.4 ± 1.1
6	5	3.8	26 ± 3.7
23	13	20.4	12 ± 1.3
24	3	2.9	15 ± 0.5
33	4	3.8	38 ± 7.7
51	4	3.1	15 ± 14
52	1	3.3	0.1 ± 0.03
54	14	12.9	14 ± 2.8
55	13	17.6	1.1 ± 0.3

^aIC₅₀ values were determined for select compounds using the RIA (see Experimental Methods for details); assays were run in duplicate at 0, 1, 3, 10, 30, 50, and 100 μM inhibitor concentration. ^b100 μM of inhibitor was used in these experiments, and the values represent the average and standard deviation of three independent measurements relative to the no inhibitor control.

Since APE1 comprises ≥95% of the total AP endonuclease activity in mammalian cells, most, if not all, of the AP site incision activity of human whole cell extracts is APE1-dependent.²⁷ Thus, as a means of assessing the specificity of candidate APE1 inhibitors and their potential biological potency, we determined the effect of the most promising actives on total AP site cleavage activity of HeLa whole cell extracts. This experiment was initially done using a single concentration of inhibitor (100 μM) to quickly establish relative activities of the selected analogues. The results showed that several compounds exhibited near 100% inhibition of the incision activity of HeLa extracts (analogues **3**, **4**, **52**, and **55**; Table 5). Taking into account the activity observed in the HTS, radiotracer, and whole cell extract assays (Table 5), we decided to pursue compounds **52** and **3** further. As such, these two compounds were tested again in the HeLa whole cell extract assay at five different concentrations (0, 1, 3, 10, 30, and 100

μM ; Figure 2). Notably, each compound was found to inhibit total AP site incision activity with IC_{50} values comparable to the

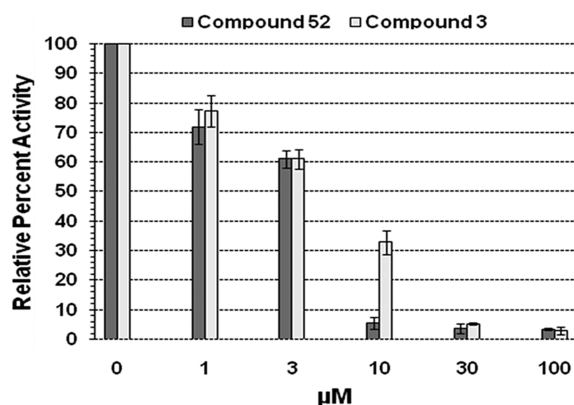


Figure 2. Inhibition of HeLa whole cell extract AP site incision activity with 3 or 52. HeLa whole cell extract (300 ng) was incubated with 0, 1, 3, 10, 30, or 100 μM indicated inhibitor at room temperature for 15 min, prior to the addition of 0.5 pmol of radiolabeled AP-DNA substrate. The reaction was then carried out at 37 $^{\circ}\text{C}$ and analyzed as described in Experimental Methods. Shown is a bar graph reporting the relative percent incision activity in comparison to the no inhibitor control, arbitrarily set at 100%. The values represent the averages and standard deviation of three independent experimental data points.

IC_{50} obtained with the purified enzyme. In particular, compound 52 showed almost complete inhibition at 10 μM , suggesting selectivity for APE1 even amidst the other nonspecific proteins of the extract.

Mechanism of APE1 Inhibition by Compounds 3 and 52. Encouraged by the potency of compound 52 in the radiotracer incision and whole cell extract assays, we pursued mechanism of action studies of this compound and our initial lead molecule 3. To reveal the mode of inhibition, we determined the kinetic parameters for APE1 incision in the absence or presence of 5, 10, or 20 μM inhibitor at varying concentrations of DNA substrate. Figure 3 shows the Michaelis–Menten plots, as well as the K_M and k_{cat} values

(determined from Lineweaver – Burk plots), of these experiments. In both cases, the k_{cat} decreases less than 6-fold, and only at the high inhibitor concentration. In the case of 52, K_M increases substantially (up to 10-fold), while the K_M increases less dramatically with 3 (up to ~ 4 -fold). Such trends would suggest that these compounds act as competitive inhibitors of APE1 activity and, thus, presumably bind the active site of the enzyme.

To further explore the potential mechanism of action of the inhibitor compounds, a previously established electrophoretic mobility shift assay (EMSA) was employed to determine the consequence of 3 and 52 on APE1 and ^{32}P radiolabeled AP-DNA complex formation and stability. The results with both inhibitors, which in the initial experiments were preincubated with the protein prior to substrate addition, showed that the percentage of APE1-DNA complex (C) decreased in a compound-dose-dependent manner (Figure 4). In particular, the binary complex was essentially absent when the protein was pretreated with 30 μM inhibitor, with compound 52 exhibiting a slightly more reproducible, greater effect. If we preincubated either of the inhibitors with the radiolabeled DNA substrate prior to the addition of APE1, we similarly saw a significant reduction in protein–DNA complex formation (Supporting Information Figure 1). Not surprisingly, a >30 -fold excess of cold (unlabeled) AP-DNA essentially abolished the formation of radiolabeled substrate complex (Supporting Information Figure 1). These data suggest that the small molecules bind the same site on APE1 as the DNA substrate (albeit apparently with lesser affinity than AP-DNA itself), thereby acting as competitive inhibitors, although an allosteric effect cannot be ruled out in the absence of high resolution complex structural information. Moreover, it is currently unknown whether these inhibitors affect other activities of APE1, such as its redox function.

Cellular Effects of APE1 Inhibitors 3 and 52. To better assess the biological potency of 3 and 52, we measured the level of genomic AP sites in MMS-treated HeLa cells with or without exposure to these compounds (Figure 5). As one might predict, treatment of cells with the alkylator MMS or either of the APE1 inhibitors alone resulted in a statistically significant increase in

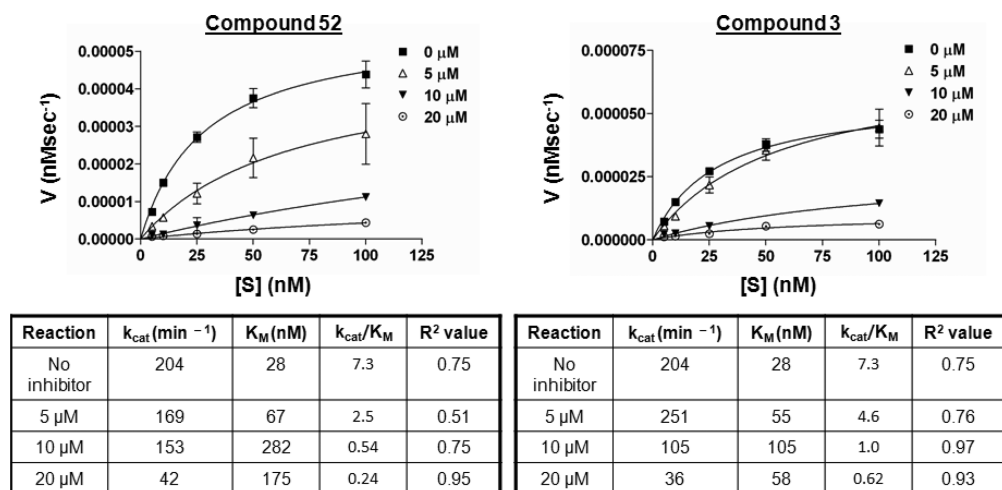


Figure 3. Kinetic analysis for compounds 3 and 52. APE1 (~ 28 pM) was incubated without or with 5, 10, or 20 μM indicated inhibitor at room temperature in RIA buffer for 15 min. Varying concentrations of ^{32}P radiolabeled AP-DNA substrate (i.e., 5, 10, 25, 50, or 100 nM) were then added, and the reactions were performed and analyzed as described in Experimental Methods. Shown are the Michaelis–Menten plots of V vs $[S]$, reporting the averages and standard deviations of at least seven data points for each value.

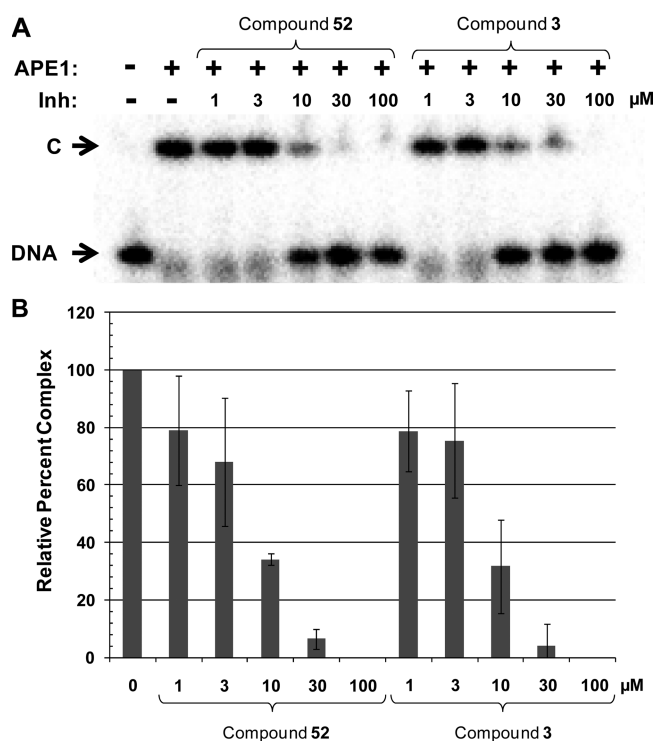


Figure 4. Stability of the APE1-DNA substrate complex in the presence of 52 or 3. (A) Representative EMSA. APE1 (~ 28 nM) was incubated without inhibitor (“-”) or with the indicated inhibitor concentration (1, 3, 10, 30, or 100 μM) for 10 min on ice. An amount of 100 fmol of abasic DNA substrate (10 nM) was then added, and the binding mixture was incubated on ice for an additional 5 min. Samples were subjected to nondenaturing polyacrylamide gel electrophoresis to separate the APE1-DNA complex (C) from unbound radiolabeled DNA (DNA). Inh = inhibitor. (B) Relative complex formation without (“0”) or with the indicated inhibitor (in μM). Shown is the average and standard deviation of three independent experimental data points, all relative to the APE1 control, without inhibitor.

the total number of AP sites relative to the DMSO control. More notably, combined treatment of MMS with either of the inhibitors resulted in a greater than additive increase (~ 3 -fold)

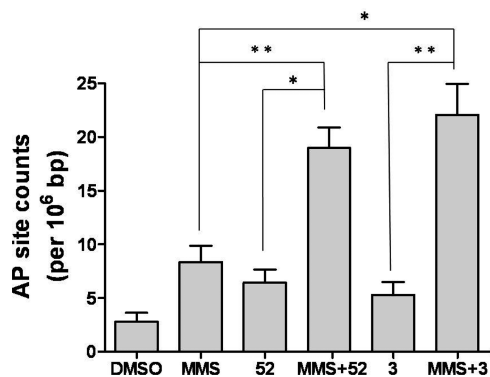


Figure 5. AP site accumulation assay. AP site counts were measured in HeLa cells after treatment with MMS and compounds alone and in combination. To evaluate inhibition of APE1 by selected compounds in cells, AP site formation was measured using the ARP assay in triplicate (see Experimental Methods). The p values were determined for an n using the Student's t test, where 3, 52, and MMS are compared with 3 and 52 alone (**, $p \leq 0.001$) and MMS alone (*, $p \leq 0.01$).

in AP sites, providing evidence that these compounds do indeed inhibit APE1 catalyzed repair of abasic damage in cells. Next, we assessed the ability of these compounds to potentiate the cytotoxic effects of MMS and TMZ in a dose-response experiment using HeLa cells and monitoring cell viability using a high-throughput luminescence-based detection of the cells' ATP content, as shown in Figure 6. Both compounds greatly potentiated the activity of these agents with optimal synergy occurring at 5–10 μM for 3 and at 10–15 μM for 52. However, compound 3 appears more cytotoxic against HeLa cells as a single agent than analogue 52, with a 50% reduction in cell viability occurring at ~ 15 and ~ 30 μM , respectively (see Supporting Information Figure 2 for a semilog plot of these data). Similar potentiation trends were observed when cell viability was monitored through a more traditional method using staining for live cells (Supporting Information Figure 3).

PK Properties of 3 and 52. Given that 3 and 52 exhibit a tractable SAR, on-target APE1 inhibition, and potentiation of the toxicity of MMS and TMZ in cell culture experiments, we were eager to assess the pharmacokinetic (PK) properties of these top compounds (Table 6). As shown in the *in vitro* absorption, distribution, metabolism, and excretion (ADME) data, both compounds 3 and 52 have many desirable attributes, yet a few liabilities. Specifically, analogue 52 exhibits improved kinetic solubility and Caco-2 permeability relative to the original lead 3. Both compounds possess favorable cell permeability and do not appear to be susceptible to active transport as shown by the efflux ratios of ~ 1 . However, compound 52 was found to be rapidly metabolized by mouse liver microsomes ($T_{1/2} = 7.8$ min), whereas compound 3 shows favorable stability ($T_{1/2} = 80$ min). These results suggest that the general core scaffold is metabolically stable, and through additional structural modifications, the potential metabolic liability of 52 could be addressed while maintaining potency. Surprisingly, as described below, we found 52 had a reasonable PK profile despite the apparent metabolic liability. Finally, both compounds exhibited some inhibition of CYP isozymes (CYP2D6 and/or CYP3A4) at 10 μM . Compound 3, which possesses substituted nitrogen (isopropyl group) and is a six-membered ring rather than five-membered, shows no inhibition of CYP2D6 at 10 μM . This result suggests that a more expansive look at all the analogues described herein may uncover structure-property relationships that obviate CYP inhibition.

The two lead compounds (52 and 3) were analyzed for their *in vivo* PK properties (Table 7) via intraperitoneal (ip) administration at 30 mg/kg body weight in 6–8 week old CD1 mice. Both compounds were well tolerated by the animals, with no adverse effects noted after a 24 h observation. Compound 52, the more hydrophilic analogue ($\text{CLogP} \approx 1$), had a favorable plasma $t_{1/2}$ of 5 h and a drug concentration (ng/mL) that exceeded the IC_{50} for over 12 h. This compound also had reasonable blood-brain barrier (BBB) penetration, with a high initial concentration that quickly tailed off, resulting in a brain/plasma (B/P) ratio of 1.4. In contrast, analogue 3, which is more lipophilic ($\text{CLogP} = 2.8$), crosses the BBB quite readily, giving rise to a B/P ratio of 21. This result correlates with expectations, as reduction of hydrogen bond donors and increased lipophilicity often lead to improved BBB penetration. The ability to modulate the BBB penetration capacity of these molecules through structural modifications could prove to be useful depending on the cancer one is targeting.

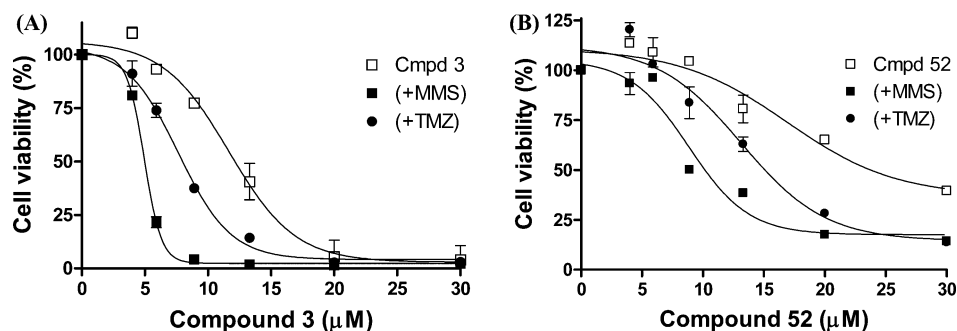


Figure 6. HeLa cell viability assay with **3** or **52** alone, in combination with either MMS (0.4 mM) or TMZ (1 mM). (A) Combined treatment of the HeLa cells with **3** at concentrations shown in the plot in the presence of 0.4 mM MMS and 1 mM TMZ. (B) Combined treatment of the HeLa cells with **52** in the presence of 0.4 mM MMS and 1 mM TMZ (see Experimental Methods). The viability values are normalized to 100% for each alkylating agent in the absence of compound. The assay was performed in triplicate.

Table 6. In Vitro ADME Properties of Lead Molecules (**3** and **52**)^a

compd	aq kinetic sol. (PBS at pH 7.4) (μM)	CYP2D6, inh at 10 μM (%)	CYP3A4, inh at 10 μM (%)	Caco-2, P_{app} 10^{-6} m/s at pH 7.4	efflux ratio (B \rightarrow A)/(A \rightarrow B)	mouse liver microsome stability, $T_{1/2}$ (min)	PBS pH 7.4 stability: % remaining after 48 h	mouse plasma stability, $T_{1/2}$ (min)
52	51.6	39	50	6.8	0.8	7.8	100	213
3	20.4	0	53	5	1.1	80	100	>250

^aAll experiments were conducted by Shanghai Chempartner Co. Ltd., and values are the average of two experiments.

Table 7. In Vivo PK data^a

compd	$t_{1/2}$ (h) [plasma]	$t_{1/2}$ (h) [brain]	[brain/plasma] ^b	C_{max} (μM) [plasma]	C_{max} (μM) [brain]	t_{max} (h) [plasma]	t_{max} (h) [brain]	CLogP ^c
52	5	2.5	1.35	36	92	0.25	0.25	1.02
3	2.1	1	21	16	217	0.25	0.25	2.83

^aExperiments were conducted at Pharmaron Inc. The ip administration (30 mpk) of CD1 male mice ($n = 3$) was monitored at eight time points (0.25, 0.5, 1, 2, 4, 8, 12, 24 h). Compound **52** was formulated as 50% PEG 200 and 10% Cremophor EL in saline solution, and compound **3** was formulated as 50% PEG 400 and 10% Cremophor EL in saline suspension. ^bCalculated based on the average B/P ratio over eight time points (24 h period). ^cCLogP values were obtained using ChemDraw Ultra 10.0.

CONCLUSION

While the work described herein did not lead to a tremendous improvement in the potency of the initial “hit” molecule **3**, it does provide valuable insights into the SAR profile of this chemotype and represents the first reported medicinal chemistry optimization campaign toward the establishment of a novel APE1 inhibitor. In particular, this effort led to the development of compounds with low single-digit micromolar potency against the purified enzyme (noticeably more potent than prior reported inhibitors), desirable in vitro and in vivo ADME properties, and the capacity to potentiate the cytotoxicity of relevant DNA-damaging agents, namely, MMS and TMZ. On-target evidence was supported by the comparable IC_{50} values against the purified recombinant APE1 protein and human whole cell extracts, as well as by increased genomic AP site accumulation in HeLa cells treated with inhibitors alone. Analysis of the in vivo PK properties of **52** and **3** in mice revealed that analogue **52** has a better general cytotoxicity profile, higher exposure levels, and a more favorable $t_{1/2}$ in the plasma, whereas compound **3** crosses the BBB more efficiently. Thus, for tumors outside the brain cavity, a compound like **52**, which does not efficiently cross the BBB, would be useful in avoiding potential complications associated with this vital organ. However, APE1 has been found to be overexpressed in adult and pediatric gliomas, with an increase in AP endonuclease activity of between 5- and 10-fold.²⁸ This observation indicates the need for the development

of APE1 inhibitors, such as **3** or other lipophilic analogues of **52**, that efficiently cross the BBB and can potentially be used in combination with a drug like TMZ. Our current efforts are focused on defining the efficacy of this class of compounds in vivo using mouse xenograft models in combination therapy with TMZ and other relevant DNA-damaging cancer chemotherapeutics.

EXPERIMENTAL METHODS

General Chemistry. Unless otherwise stated, all reactions were carried out under an atmosphere of dry argon or nitrogen in dried glassware. Indicated reaction temperatures refer to those of the reaction bath, while room temperature (rt) is noted as 25 °C. All solvents were of anhydrous quality purchased from Sigma Chemical Co. and used as received. Commercially available starting materials and reagents were purchased from Sigma and were used as received.

Analytical thin layer chromatography (TLC) was performed with Sigma Aldrich TLC plates (5 cm \times 20 cm, 60 Å, 250 μm). Visualization was accomplished by irradiation under a 254 nm UV lamp. Chromatography on silica gel was performed using forced flow (liquid) of the indicated solvent system on Biotage KP-Sil prepacked cartridges and using the Biotage SP-1 automated chromatography system. ¹H and ¹³C NMR spectra were recorded on a Varian Inova 400 MHz spectrometer. Chemical shifts are reported in ppm with the solvent resonance as the internal standard (CDCl₃, 7.26 ppm, 77.00 ppm, DMSO-*d*₆, 2.49 ppm, 39.51 ppm for ¹H, ¹³C, respectively). Data are reported as follows: chemical shift, multiplicity (s = singlet, d = doublet, t = triplet, q = quartet, br = broad, m = multiplet), coupling constants, and number of protons. Low resolution mass spectra (electrospray ionization) were acquired on an Agilent Technologies

6130 quadrupole spectrometer coupled to the HPLC system. High resolution mass spectral data were collected in-house using an Agilent 6210 time-of-flight mass spectrometer, also coupled to an Agilent Technologies 1200 series HPLC system. If needed, products were purified via a Waters semipreparative HPLC instrument equipped with a Phenomenex Luna C18 reverse phase (5 μm , 30 mm \times 75 mm) column having a flow rate of 45 mL/min. The mobile phase was a mixture of acetonitrile (0.025% TFA) and H₂O (0.05% TFA), and the temperature was maintained at 50 °C.

Samples were analyzed for purity on an Agilent 1200 series LC/MS instrument equipped with a Luna C18 reverse phase (3 μm , 3 mm \times 75 mm) column having a flow rate of 0.8–1.0 mL/min over a 7 min gradient and a 8.5 min run time. Purity of final compounds was determined to be >95%, using a 3 μL injection with quantitation by AUC at 220 and 254 nm (Agilent diode array detector).

RIA. Recombinant wild type APE1 protein was purified as previously described.²⁹ An amount of 50 pg of APE1 (~140 pM) was incubated without (positive control containing 1% DMSO) or with the indicated inhibitor at the indicated concentration at room temperature in RIA buffer (50 mM Tris, pH 7.5, 25 mM NaCl, 1 mM MgCl₂, 1 mM DTT, 0.01% Tween-20) for 15 min. One-half pmol of ³²P 5'-radiolabeled AP-DNA substrate (18 mer) was added to a 10 μL final volume,³⁰ and the mixtures were incubated at 37 °C for 5 min and the reactions stopped by adding stop buffer (0.05% bromophenol blue/xylene cyanol dissolved in 95% formamide, 20 mM EDTA) and heating at 95 °C for 10 min. Intact substrate was separated from incised product on a 15% polyacrylamide denaturing gel in a Tris/boric acid/EDTA buffer. Following electrophoresis, the gel was subjected to standard phosphorimager analysis using the ImageQuant 5.2 software, and the percent incision activity (amount of substrate converted to product) was calculated. IC₅₀ values (i.e., the concentration of inhibitor at which 50% inactivation was observed) were extrapolated after plotting the results of duplicate incision sets (at inhibitor concentrations ranging from 1 μM to 100 μM) and fitting data using the Hill equation in GraphPad Prism, version 4.0, software.

HeLa Whole Cell Extract Incision Assays. To prepare protein extracts, HeLa cells maintained in DMEM with 10% fetal bovine serum and 1% penicillin–streptomycin were harvested, washed with 1 \times PBS, and resuspended in ice cold hypotonic lysis buffer (50 mM Tris, pH 7.4, 1 mM EDTA, 1 mM DTT, 10% glycerol, 0.5 mM PMSF). The suspension was frozen at –80 °C for at least 30 min and then slowly thawed at 4 °C for ~1 h. KCl was added to the cell suspension to a final concentration of 222 mM, followed by incubation on ice for 30 min and clarification by centrifugation at 12000g for 15 min at 4 °C. The supernatant (whole cell extract) was retained and the protein concentration determined using the Bio-Rad Bradford reagent. Aliquots were stored until needed at –80 °C. For the incision assays, 300 ng of HeLa whole cell extract was incubated with 0, 1, 3, 10, 30, or 100 μM indicated inhibitor at room temperature for 15 min prior to the addition of 0.5 pmol of ³²P radiolabeled AP-DNA substrate (final volume of 10 μL). The reaction mix was then transferred to 37 °C for 5 min to allow for incision. Following addition of stop buffer and heat denaturation, the reaction products were analyzed as indicated above.

Enzyme Kinetic Studies. An amount of 10 pg of APE1 (~28 pM) was incubated without (positive control, 1% DMSO) or with 5, 10, or 20 μM indicated inhibitor at room temperature in RIA buffer (see above) for 15 min. Varying concentrations of ³²P radiolabeled AP-DNA substrate (i.e., 5, 10, 25, 50, or 100 nM) were then added to a 10 μL final volume. The mixtures were incubated at 37 °C for 5 min and the reactions stopped by adding stop buffer and heating at 95 °C for 10 min. The reaction velocity (nanomolar substrate incised per minute) at each substrate concentration was calculated as described above. Lineweaver – Burk plots of 1/V versus 1/[S] were used to determine K_M and k_{cat} and the mode of inhibition.

EMSA. An amount of 10 ng of APE1 (~28 nM) was incubated without inhibitor (positive control, 1% DMSO) or with increasing concentrations of inhibitor (1, 3, 10, 30, and 100 μM) in binding buffer (50 mM Tris, pH 7.5, 25 mM NaCl, 1 mM EDTA, 1 mM DTT, 10% glycerol, 0.01% Tween 20) for 10 min on ice, and then radiolabeled ³²P AP-DNA substrate (100 fmol) was added to a 10 μL

final volume. Following incubation on ice for 5 min, samples were subjected to nondenaturing polyacrylamide gel electrophoresis (20 mM Tris, pH 7.5, 10 mM sodium acetate, 0.5 mM EDTA, 8% polyacrylamide, 2.5% glycerol) for 2 h at 120 V in electrophoresis buffer (20 mM Tris, pH 7.5, 10 mM sodium acetate, 0.5 mM EDTA) to separate the APE1-DNA complex from unbound radiolabeled DNA.³¹ After electrophoresis, the gel was subjected to standard phosphorimager analysis as above, and the percentage of substrate DNA in complex with APE1 was determined.

Genomic AP Site Accumulation in Cells. HeLa cells with 80% confluency in a 25 cm² flask were treated with DMSO, 275 μM MMS, or 7.5 μM APE1 inhibitor alone or with a combination of 275 μM MMS and 7.5 μM inhibitor for 24 h at 37 °C. Cells were then harvested, and genomic DNA of each sample was isolated according to Qiagen Genomic DNA isolation kit. The concentration of genomic DNA was measured and adjusted to 100 ng/ μL . An amount of 10 μL of purified DNA was further labeled with an aldehyde reactive probe (ARP) reagent (*N*'-aminooxymethylcarbonylhydrazino-D-biotin), and AP sites were measured using the DNA damage quantification kit from Dojindo Molecular Technologies.

MMS and TMZ Potentiation Assay. HeLa cells were plated by multichannel pipet or Multidrop Combi dispenser (Thermo) at 6K/25 μL per well in DMEM culture medium with 10% FBS into white solid bottom 384-well cell culture plates. Cells were cultured at 37 °C overnight to allow for cell attachment. The following day, the entire cell medium in the well was replaced with fresh medium containing serial dilutions of the compounds of interest (5–30 μM) in the presence or absence of MMS (0.4 mM) or TMZ (1 mM). The plates were incubated for 24 h at 37 °C. Cell viability was then evaluated via luminescence detection by adding 15 μL of CellTiter Glo reagent (Promega, Madison, WI) to each well and incubating at room temperature for 30 min and subsequently measuring the luminescence using a ViewLux reader. Percent viability was calculated for each concentration of the tested compounds in duplicate relative to the luminescence of the negative DMSO control.

In Vivo PK Analysis. Compound 3 was dissolved in PEG 400 and Cremophor with vortexing and sonification. Then saline was gradually added with vortexing and sonification to obtain a final concentration of 3 mg/mL 3 in 50% PEG 400 and 10% Cremophor. Compound 52 was dissolved in PEG 200 Cremophor with vortexing and sonification. Then saline was gradually added as above to obtain a final concentration of 3 mg/mL 52 in 50% PEG 200 and 10% Cremophor. The dose for both compounds was administered ip. All blood samples were collected through a cardiac puncture per sampling time point (0.25, 0.5, 1, 2, 4, 8, 12, and 24 h postdose). Approximately 0.12 mL of blood was collected at each time point. All blood samples were transferred into plastic microcentrifuge tubes containing heparin and placed at –80 °C until processed (see below). At each time point (see above), the brain was harvested immediately after euthanasia by carbon dioxide. The brain was rinsed with saline and wiped clean and then weighed in a sterilized plastic tube. The tissue sample was then homogenized in water with a brain weight (g) to water (mL) ratio of 1:4 (g:mL). The detected values were then multiplied by 5 to achieve the final concentration of the compound in the brain. Blood samples were processed for plasma by centrifugation at 4 °C at 4000g for 5 min. Plasma samples were then stored in tubes, quickly frozen in a freezer, and kept at –80 °C until LC/MS/MS analysis. Plasma concentration of compound 3 or 52 at the various time points (data obtained from the LC/MS/MS studies) was analyzed using the WinNonlin software program.

■ ASSOCIATED CONTENT

Supporting Information

Additional experimental procedures and ¹H, LC/MS, and HRMS data for representative compounds. This material is available free of charge via the Internet at <http://pubs.acs.org>.

AUTHOR INFORMATION

Corresponding Author

*For D.J.M.: phone, 301-217-4381; fax, 301-217-5736; e-mail, maloneyd@mail.nih.gov. For D.M.W.: phone, 410-558-8153; fax, 410-558-8157; e-mail, wilsonda@mail.nih.gov.

Author Contributions

[§]These authors contributed equally to this work.

Notes

The authors declare no competing financial interest.

ACKNOWLEDGMENTS

The authors thank William Leister, Paul Shinn, Danielle VanLeer, James Bougie, and Tom Daniel for assistance with compound management and purification. We also thank Christina Greco for critical reading of the manuscript and technical assistance. This research was supported by the Intramural Research Program of the NIH, National Institute on Aging, as well as by the NIH Grant R03 MH086444-01 (D.M.W.), and the Molecular Libraries Initiative of the National Institutes of Health Roadmap for Medical Research.

ABBREVIATIONS USED

APE1, apurinic/apyrimidinic endonuclease 1; HTS, high-throughput screening; qHTS, quantitative high-throughput screening; MLSMR, Molecular Libraries Small Molecule Repository; BER, base excision repair; ML199, *N*-(3-(benzo[*d*]thiazol-2-yl)-5,6-dihydro-4*H*-thieno[2,3-*c*]pyrrol-2-yl)-acetamide; TMZ, temozolomide; RIA, radiotracer incision assay; ADME, absorption, distribution, metabolism, and excretion; dppp, 1,3-bis(diphenylphosphino)propane; xantphos, 4,5-bis(diphenylphosphino)-9,9-dimethylxantene; dba, dibenzylidene acetone; EDC, 1-ethyl-3-(3-dimethylaminopropyl)carbodiimide; HATU, 2-(1*H*-7-azabenzotriazol-1-yl)-1,1,3,3-tetramethyluronium hexafluorophosphate; MMS, methylmethane sulfonate

REFERENCES

- (1) Wilson, D. M. III; Barsky, D. The major human abasic endonuclease: formation, consequences and repair of abasic lesions in DNA. *Mutat. Res.* **2001**, *485*, 283–307.
- (2) Demple, B.; Sung, J. S. Molecular and biological roles of Ape1 protein in mammalian base excision repair. *DNA Repair* **2005**, *4*, 1442–1449.
- (3) Robertson, A. B.; Klungland, A.; Rognes, T.; Leiros, I. DNA repair in mammalian cells: base excision repair: the long and short of it. *Cell. Mol. Life Sci.* **2009**, *66*, 981–993.
- (4) Wilson, D. M. III. Processing of nonconventional DNA strand break ends. *Environ. Mol. Mutagen.* **2007**, *48*, 772–782.
- (5) Tell, G.; Quadrioglio, F.; Tiribelli, C.; Kelley, M. R. The many functions of APE1/Ref-1: not only a DNA repair enzyme. *Antioxid. Redox. Signaling* **2009**, *11*, 601–620.
- (6) Bhakat, K. K.; Mantha, A. K.; Mitra, S. Transcriptional regulatory functions of mammalian AP-endonuclease (APE1/Ref-1), an essential multifunctional protein. *Antioxid. Redox. Signaling* **2009**, *11*, 621–638.
- (7) Luo, M.; He, H.; Kelley, M. R.; Georgiadis, M. M. Redox regulation of DNA repair: implications for human health and cancer therapeutic development. *Antioxid. Redox. Signaling* **2010**, *12*, 1247–1269.
- (8) Bapat, A.; Fishel, M. L.; Kelley, M. R. Going ape as an approach to cancer therapeutics. *Antioxid. Redox. Signaling* **2009**, *11*, 651–668.
- (9) Abbotts, R.; Madhusudan, S. Human AP endonuclease 1 (APE1): from mechanistic insights to druggable target in cancer. *Cancer Treat. Rev.* **2010**, *36*, 425–435.

(10) Mutter, N.; Stupp, R. Temozolomide: a milestone in neuro-oncology and beyond? *Expert Rev. Anticancer Ther.* **2006**, *6*, 1187–1204.

(11) Rouleau, M.; Patel, A.; Hendzel, M. J.; Kaufmann, S. H.; Poirier, G. G. PARP inhibition: PARP1 and beyond. *Nat. Rev. Cancer* **2010**, *10*, 293–301.

(12) Petermann, E.; Helleday, T. Pathways of mammalian replication fork restart. *Nat. Rev. Mol. Cell Biol.* **2010**, *11*, 683–687.

(13) (a) Bryant, H. E.; Schultz, N.; Thomas, H. D.; Parker, K. M.; Flower, D.; Lopez, E.; Kyle, S.; Meuth, M.; Curtin, N. J.; Helleday, T. Specific killing of BRCA2-deficient tumors with inhibitors of poly(ADP-ribose) polymerase. *Nature* **2005**, *434*, 913–917. (b) Farmer, H.; McCabe, N.; Lord, C. J.; Tutt, A. N. J.; Johnson, D. A.; Richardson, T. B.; Santarosa, M.; Dillon, K. J.; Hickson, I.; Knights, C.; Martin, N. M. B.; Jackson, S. P.; Smith, G. C. M.; Ashworth, A. Targeting the DNA repair defect in BRCA mutant cells as a therapeutic strategy. *Nature* **2005**, *434*, 917–921.

(14) Guha, M. PARP inhibitors stumble in breast cancer. *Nat. Biotechnol.* **2011**, *29*, 373–374.

(15) Wilson, D. M. III; Simeonov, A. Small molecule inhibitors of DNA repair nuclease activities of APE1. *Cell. Mol. Life Sci.* **2010**, *67*, 3621–3631.

(16) Bapat, A.; Glass, L. S.; Luo, M.; Fishel, M. L.; Long, E. C.; Georgiadis, M. M.; Kelley, M. R. Novel small molecule inhibitor of APE1 endonuclease blocks proliferation and reduces viability of glioblastoma cells. *J. Pharmacol. Exp. Ther.* **2010**, *334*, 988–998.

(17) Madhusudan, S.; Smart, F.; Shrimpton, P.; Parsons, J. L.; Gardiner, L.; Houlbrook, S.; Talbot, D.; Hammonds, T.; Freemont, P. A.; Sternberg, M. J. E.; Dianov, G. L.; Hickson, I. D. Isolation of a small molecule inhibitor of DNA base excision repair. *Nucleic Acids Res.* **2005**, *33*, 4711–4724.

(18) Fishel, M. L.; Kelley, M. R. The DNA. Base excision repair protein APE1/Ref-1 as a therapeutic and chemopreventive target. *Mol. Aspects Med.* **2007**, *28*, 375–395.

(19) Mohammed, M. Z.; Vyjayanti, V. N.; Laughton, C. A.; Dekker, L. V.; Fischer, P. M.; Wilson, D. M. III; Abbotts, R.; Shah, S.; Patel, P. M.; Hickson, I. D.; Madhusudan, S. *Br. J. Cancer* **2011**, 1–11.

(20) Zawahir, Z.; Dayam, R.; Deng, J.; Pereira, C.; Neamati, N. Pharmacophore guided discovery of small-molecule human apurinic/apyrimidinic endonuclease APE1. *J. Med. Chem.* **2009**, *52*, 20–32.

(21) (a) Bases, R. E.; Mendez, F. Topoisomerase inhibition by luanthone, an adjuvant in radiation therapy. *Int. J. Radiat. Oncol., Biol., Phys.* **1997**, *37*, 1133–1137. (b) Luo, M.; Kelley, M. R. Inhibition of the human apurinic/apyrimidinic endonuclease (APE1) repair activity and sensitization of breast cancer cells to DNA alkylating agents with luanthone. *Anticancer Res.* **2004**, *24*, 2127–2134.

(22) (a) Taverna, P.; Liu, L.; Hwang, H. S.; Hanson, A. J.; Kinsella, T. J.; Gerson, S. L. Methoxyamine potentiates DNA single strand breaks and double strand breaks induced by temozolomide in colon cancer cells. *Mutat. Res.* **2001**, *485*, 269–281. (b) Fishel, M. L.; He, Y.; Smith, M. L.; Kelley, M. R. Manipulation of base excision repair to sensitize ovarian cancer cells to alkylating agent temozolomide. *Clin. Cancer Res.* **2007**, *13*, 260–267.

(23) Seiple, L. A.; Cardellina, J. H. 2nd; Akee, R.; Stivers, J. T. Potent inhibition of human apurinic/apyrimidinic endonuclease 1 by arylstilbonic acids. *Mol. Pharmacol.* **2008**, *73*, 669–677.

(24) Simeonov, A.; Kulkarni, A.; Dorjsuren, D.; Jadhav, A.; Shen, M.; McNeill, D. R.; Austin, C. P.; Wilson, D. M. 3rd. Identification and characterization of inhibitors of human apurinic/apyrimidinic endonuclease APE1. *PLoS One* **2009**, *4*, e5740.

(25) These compounds are a part of the NIH Small Molecule Repository; see <http://mli.nih.gov/mli/compound-repository/mlsmr-compounds/>.

(26) (a) Gwald, K.; Schinke, E.; Boettcher, H. 2-Amino-thiophene aus methylenaktiven nitrile carbonylverbindungen und schwefel. *Chem. Ber.* **1966**, *99*, 94–100. (b) Andersen, H. S.; Olsen, O. H.; Iversen, L. F.; Sorensen, A. L. P.; Mortensen, S. B.; Christensen, M. S.; Branner, S.; Hansen, T.; Lau, J. F.; Jeppesen, L.; Moran, E. J.; Su, J.; Bakir, F.; Judge, L.; Shahbaz, M.; Collins, T.; Vo, T.; Newman, M. J.

Ripka, W. C.; Moller, N. P. H. Discovery and SAR of a novel selective and orally bioavailable nonpeptide classical competitive inhibitor class of protein-tyrosine phosphatase 1B. *J. Med. Chem.* **2002**, *45*, 4443–4459.

(27) Demple, B.; Harrison, L. Repair of oxidative damage to DNA: enzymology and biology. *Annu. Rev. Biochem.* **1994**, *63*, 915–948.

(28) Bobola, M. S.; Blank, A.; Berger, M. S.; Stevens, B. A.; Silber, J. R. Apurinic/aprimidinic endonuclease activity is elevated in human adult gliomas. *Clin. Cancer Res.* **2001**, *7*, 3510–3518.

(29) Erzberger, J. P.; Barsky, D.; Scharer, O. D.; Colvin, M. E.; Wilson, D. M. III. Elements in abasic site recognition by the major human and *Escherichia coli* apurinic/aprimidinic endonucleases. *Nucleic Acids Res.* **1998**, *26*, 2771–2778.

(30) Wilson, D. M. III; Takeshita, M.; Grollman, A. P.; Demple, B. Incision activity of human apurinic endonuclease (Ape) at abasic site analogs in DNA. *J. Biol. Chem.* **1995**, *270*, 16002–16007.

(31) Wilson, D. M. III; Takeshita, M.; Demple, B. Abasic site binding by the human apurinic endonuclease, Ape, and determination of the DNA contact sites. *Nucleic Acids Res.* **1997**, *25*, 933–939.